Error Analysis of Planar Ion Crystals and Ion Chains Implementing the Bacon–Shor Code

Cheng-Yu Liu[1*] Ming-Chin Ho[1]

[1] *Department of Physics, National Taiwan University, Taipei, Taiwan*

Introduction

Implementations of Bacon–Shor codes on a 23-ion chain have been reported in [1]. Building on this, we explore extensions to two-dimensional ion crystals, considering mode frequencies and participation, and noting possible performance degradation in 2D.
We identify random heating as a main source of gate errors and propose using far-detuned optical tweezers [2] to provide local confinement, thereby tailoring mode frequencies and potentially improving gate performance [7].
Finally, we simulate Bacon–Shor codes and extract decoders from the corresponding syndromes. Future work will include incorporating gate and heating errors into full error-correction circuits and exploring possible more complex error codes in ion chains, planes, and 3D arrays.

Ion Chain Setup

The experiment drive the radial modes of an 23 ions ion chain to couple ions.

→From [1], Fig. (a) shows the corresponding 23 modes and the frequencies of state-dependent amplitude-modulated forces.
→From [1], Fig. (b) shows the corresponding 23 modes decay parameter $\epsilon_i(t=0) = \frac{(b_i)^2 hn(t=0)}{m(\omega_0)^2\omega}$ = which are used to characterize the error caused by ions motion inside the Gaussian laser beam.

(a) Graph from [1]

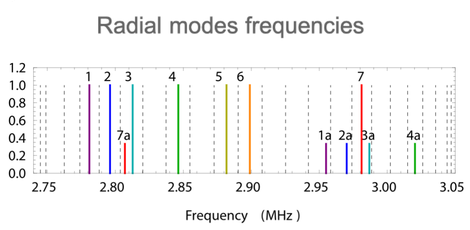

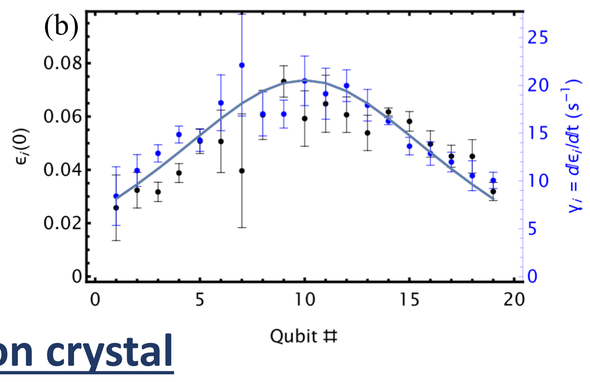

Planar Ion crystal

Objective

→Based on the 1D ion chain parameters in [3], we study a 2D ion crystal to check if more complex ion arrangements can reduce heating (stronger secular frequencies suppress heating error) and enhance gate speed [4].

Equlibrium, out-of plane modes, and in-plane normal modes

Here we consider first case with secular frequency along three directions $\omega_x = 0.18 \times 2\pi$ MHz, $\omega_y = 0.22 \times 2\pi$ MHz, $\omega_z = 2.21 \times 2\pi$ MHz [2] for Fig. (c). Fig. (d) and Fig. (e) shows two times and four times stronger of the three directions secular frequency compared with the first case (Fig. (c))
→Note that the secular frequency is increased by assuming stronger AC/DC voltages and a higher RF drive. However, the configuration shown in Fig. (e) may not be experimentally feasible at present.

(c) (d) (e)

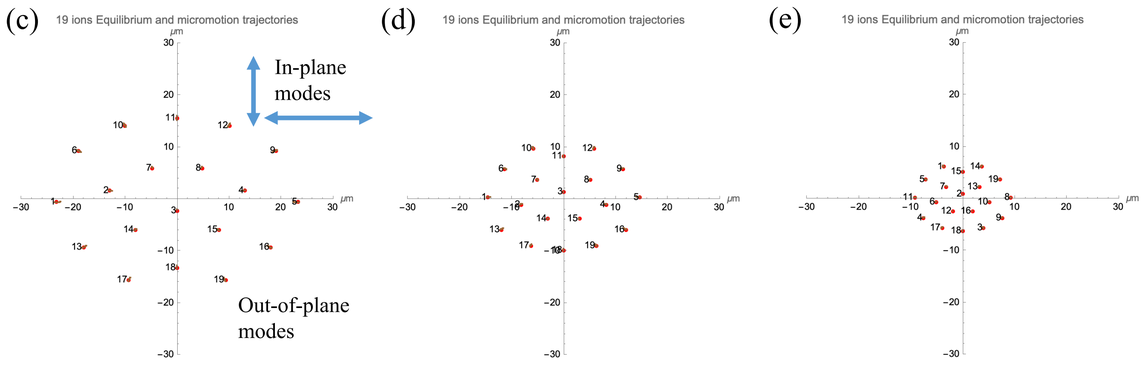

→From Fig. (a), (b), and (c), we observe that the micromotion amplitudes (brown trajectories) are suppressed by stronger trapping frequencies.
→The ion separations are around 4 μm shown in Fig. (c), which is comparable to the values reported in [1]. However, in ion crystal, this requires extreme strong AC and DC potential.

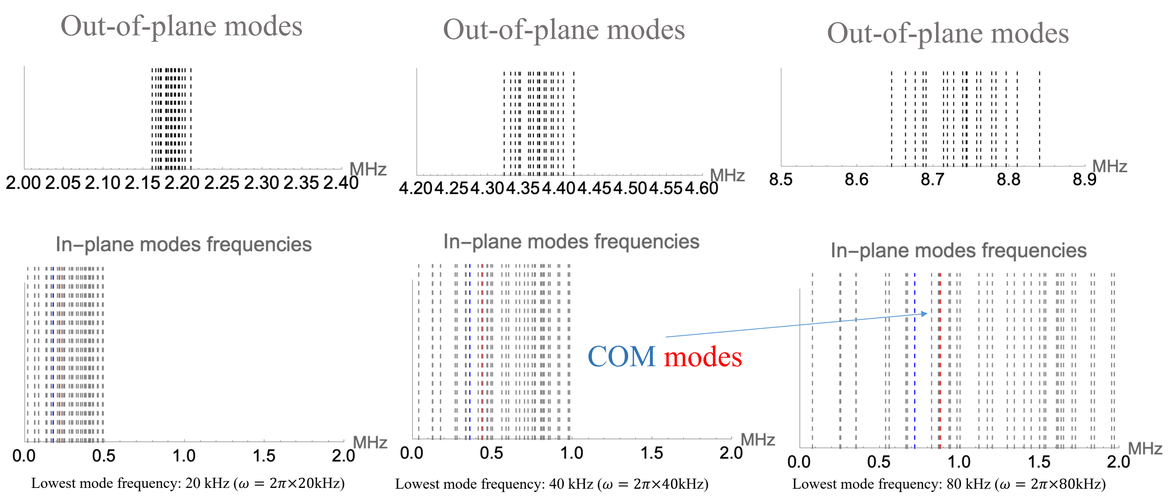

→ Out-of plane modes can be less packed and increased if increasing trapping frequencies. If perform entangling gate on out-of plane modes, then higher secular frequencies could benefit the gate speed.
→ Lowest in-plane mode frequency can be increased by increasing in-plane trapping frequencies, however, the lowest mode frequency are extremly lower than the secular frequency. This means 2D ion crystal are easily suffered from heating problem.
→ Even with the most extreme case Fig. (e), , micromotion amplitude is still comparable with heating motion in 1D ion chain. However, micromotion is deterministic which can be further designed [5]

→ Below shows the participation b_i of the lowest in-plane mode in color map, here we define $b_i = \sqrt{b_{ix}^2 + b_{iy}^2}$.
→ A uniform increase in the trapping frequencies along all three directions leave the participation factors b_i unchanged. Hence, in Fig. (a) (b) (c), the dots appear with identical colors but shifted equlibrium positions

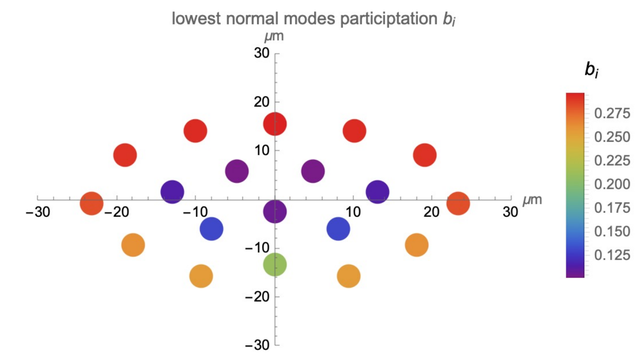

→ Participation b_i shown here provides us the way to engineer the laser field for heating error in 2D ion crystal, as in [1] and next section, we could design laser pulse based on different couplings (b_i) from ith to the lowest mode.

Effects of adding dipole force during gate implementations

→We first estimate the gate error pointed out in [1], this could be calculated by using decay parameter ϵ_i as shown in Fig. (b). Other parameters given are $n(t=0) = 660$ phonons, $m = 171u$ (Yb^+), axial frequency $\omega = 2\pi\times174$MHz, beam waist $\omega_0 = 450$nm.

→Here we calculate an anharmonic potential [6] look like $V = \frac{1}{2}mx^2\omega^2 + \frac{1.1}{2}mx^4\omega^2$ to obtain b_i so we could arrive at Fig. (f) the similar decay parameter as shown in Fig. (b) (From experiment).

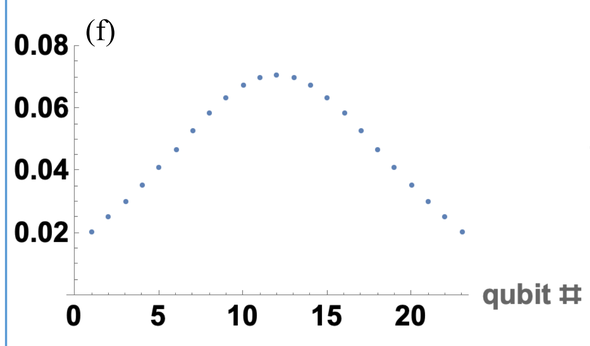

→ $\epsilon_i(t=0) = \frac{(b_i)^2 hn(t=0)}{m(\omega_0)^2\omega} = 0.02\sim0.07$

Gate error modeling

→ We take ion 4 and ion 8 with $b_4 \approx 0.180$, $b_8 \approx 0.239$ and we have actual single-qubit rotation and two-qubit rotation angle $\tilde{\theta}$ (assume $n(t) = 800$) :

$$\tilde{\theta} = \theta(1+\epsilon_i(0))f(\epsilon_i(t)) = \theta(1+\epsilon_i(0))e^{-\epsilon_i(t)}I_0(\epsilon_i(t)) = 0.9923\theta \text{ (two-qubit: } 0.977\ \theta)$$

Desired rotation angle — Designed compensation — Error from thermal motion

→ If consider adding local tweezer driving off resonance between $S_{1/2} \to P_{1/2}$ (369.5 nm) by wavelength 1070nm, waist μm, power $1W$. Then local trap frequencies ω_l can be 200 kHZ with scattering rate $S = 2s^{-1}$[2]. We apply the trapping field to ions 1, 2, 14, 22, and 23. This process tailor the chain frequency and rearrange ion participation b_i [7]. We then calculate ion 4 single qubit and ion 4 and ion 8 two-qubit rotations:

$$\tilde{\theta} = \theta(1+\epsilon_i(0))f(\epsilon_i(t)) = \theta(1+\epsilon_i(0))e^{-\epsilon_i(t)}I_0(\epsilon_i(t)) = 0.9928\theta \text{ (two-qubit: } 0.980\ \theta)$$

→ Further, we can rearrange these tweezered ions to 5, 9, 11, 14 ,17 . We then apply above same conditions (Noted this time axial frequency is enhanced to $\omega = 2\pi\times202$MHz.) to have qubit rotations:

$$\tilde{\theta} = \theta(1+\epsilon_i(0))f(\epsilon_i(t)) = \theta(1+\epsilon_i(0))e^{-\epsilon_i(t)}I_0(\epsilon_i(t)) = 0.993\theta \quad \text{(two-qubit: } 0.982\ \theta)$$

This demonstrates the ability of the tweezer to tailor mode frequencies and mitigate heating errors. With more ancilla qubits in the chain, qubit rotations could be performed with even higher fidelity.

Bacon-Shor codes Implementations

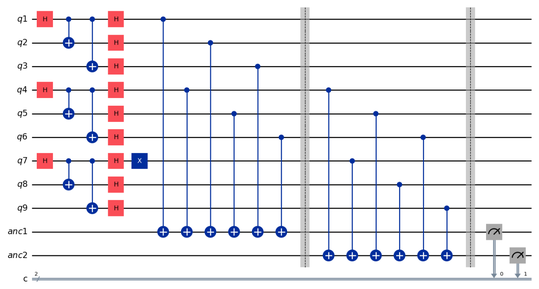

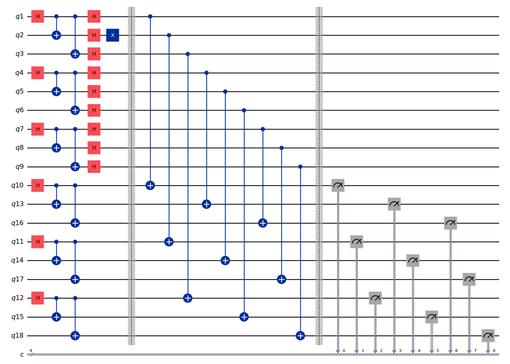

```
✓ 0.0s
syndrome (Z₁Z₂Z₃Z₄Z₅Z₆,Z₄Z₅Z₆Z₇Z₈Z₉): 01
```

→ Decoder: X_7

```
✓ 0.0s
parities elements (Z₁Z₂Z₃Z₄Z₅Z₆Z₇Z₈Z₉) : 010111000
syndrome (Z₁Z₂Z₃Z₄Z₅Z₆,Z₄Z₅Z₆Z₇Z₈Z₉): 01
```

→ Decoder: X_1

Acknowledgments

Part of this work was done while Cheng-Yu Liu was at National Taiwan University.

The author thanks advisor Guin-Dar Lin and senior Chun-Chi Lin

[1] Huang, Shilin, Kenneth R. Brown, and Marko Cetina. "Comparing Shor and Steane error correction using the Bacon-Shor code." *Science Advances* 10.45 (2024): eadp2008.
[2] Arias Espinoza, Juan Diego, et al. "Engineering spin-spin interactions with optical tweezers in trapped ions." *Physical Review A* 104.1 (2021): 013302.
[3] Wang, ST., Shen, C. & Duan, LM. Quantum Computation under Micromotion in a Planar Ion Crystal. *Sci Rep* **5**, 8555 (2015). https://doi.org/10.1038/srep08555
[4] Micromotion-tolerate fast entangling gates in planar trapped ion-crystal https://doi.org/10.6342/NTU202203211
[5] Hou, YH., Yi, YJ., Wu, YK. *et al.* Individually addressed entangling gates in a two-dimensional ion crystal. *Nat Commun* **15**, 9710 (2024). https://doi.org/10.1038/s41467-024-53405-z
[6] Lin, G-D., et al. "Large-scale quantum computation in an anharmonic linear ion trap." *Europhysics Letters* 86.6 (2009): 60004.
[7] Shen, Yu-Ching, and Guin-Dar Lin. "Scalable quantum computing stabilised by optical tweezers on an ion crystal." *New Journal of Physics* 22.5 (2020): 053032.

*corresponding author. email: 316497z@gmail.com.